Earth Syst. Sci. Data, 17, 5209–5219, 2025
https://doi.org/10.5194/essd-17-5209-2025


Open Access Earth System Science Data

# Data collected by a drone backpack for air quality and atmospheric state measurements during Pallas Cloud Experiment 2022 (PaCE2022)

**David Brus, Viet Le, Joel Kuula, and Konstantinos Doulgeris**

Finnish Meteorological Institute, Erik Palménin aukio 1, 00506, Helsinki, Finland

**Correspondence:** David Brus (david.brus@fmi.fi)

Received: 5 February 2025 – Discussion started: 18 February 2025
Revised: 5 June 2025 – Accepted: 14 July 2025 – Published: 9 October 2025

**Abstract.** A lightweight, custom-built drone backpack for air quality and atmospheric state variable measurements, mounted on top of consumer-grade drone, was used during the Pallas Cloud Experiment (PaCE) campaign's intensive operation period (IOP) between 12 September and 10 October 2022. The drone backpack measurements include 63 vertical profile flights from two close by locations at Pallasjärvi lake and 12 intercomparison flights against reference instrumentation at Sammaltunturi station. The observations include aerosol number concentrations and size distributions and meteorological parameters (temperature, relative humidity, pressure, and wind speed and direction) up to 500 m above ground level. The dataset has been uploaded to the common Zenodo PaCE 2022 community archive (https://zenodo.org/communities/pace2022/, last access: 5 June 2025). The datasets are available in two formats, NetCDF and CSV, from https://doi.org/10.5281/zenodo.14780929 (Brus et al. 2025a) and https://doi.org/10.5281/zenodo.14778421 (Brus et al. 2025b), respectively.

## 1 Introduction

Aerosol–cloud interactions and cloud microphysics are a weak point in all atmospheric models, regardless of resolution (e.g., Morrison et al., 2020). It has been particularly challenging to accurately represent the Arctic climate system and Arctic clouds in regional- and large-scale climate models (e.g., Sedlar et al., 2020). Cloud properties are sensitive to aerosols, which act as cloud condensation nuclei (CCN) and ice-nucleating particles (INP), especially in areas where the aerosol and CCN concentrations are low (Stevens et al., 2018). This makes the cloud properties in the Arctic and subarctic susceptible to anthropogenic pollution (e.g., Coopman et al., 2018; Liu and Li, 2019; Doulgeris et al., 2023). While there have been several large-scale efforts to characterize aerosol–cloud–climate interactions in the Central and High Arctic (e.g., Abbatt et al., 2019; Pasquier et al., 2022), the subarctic zone has received relatively little attention. However, our previous research has shown that even the relatively clean air in the Finnish subarctic is a complex mixture of potential aerosol precursors from various marine, biological, and anthropogenic sources and that changes in anthropogenic emissions can have an impact on subarctic aerosol. For example, one of the largest sources of anthropogenic atmospheric $SO_2$ in Finnish Lapland was is smelter industry on the Kola Peninsula (Asmi et al., 2011; Kyrö et al., 2014; Jokinen et al., 2022). The relative contributions of different aerosol sources in the Arctic and subarctic can be expected to change in response to climate change (increasing temperatures, reduced snow and ice cover, and increasing biogenic emissions) and changes in human activity (changes in long-range transport and local activities such as shipping and mining). The implications of these rapid changes currently happening in the Arctic and subarctic on aerosol–radiation interactions and low-level clouds have remained elusive (Schmale et al., 2022).

The use of uncrewed aircraft systems (UASs) to probe the atmosphere has been progressively increasing. The current UASs are relatively easy to deploy and have the advantage of frequent, high-resolution, and affordable profiling of the atmosphere. The latest efforts toward the miniaturization of instrumentation, the cost reduction of hardware, and the

availability of consumer-grade platforms have allowed atmospheric research to increasingly expand with respect to vertical dimension. Several atmospheric scientific UAS campaigns have focused on the data collection of meteorological parameters, aerosols, and clouds in the atmospheric boundary layer and at higher latitudes (e.g., Altstädter et al., 2015; de Boer et al., 2020; Kral et al., 2021; Girdwood et al., 2022).

Several studies have conducted vertical measurements of particulate matter concentrations and aerosol size distributions using different variations of heavy-lifting multicopters, equipped with off-the-shelf or custom-built instrumentation, in environments with both low and very high loads of atmospheric pollutants (e.g., Zhu et al., 2019; Liu et al., 2020; Samad et al., 2020; Brus et al., 2021; Thivet et al., 2025). Over the last 2 decades, the Finnish Meteorological Institute (FMI) has conducted extensive research on aerosol–cloud interactions within the framework of the targeted Pallas Cloud Experiment (PaCE) campaign, focused on different phenomena, covering sources of precursors for new particle formation, aerosol chemistry, CCN activation, in situ cloud measurements, and remote-sensing and satellite observations. During PaCE 2022, several airborne platforms were deployed simultaneously to determine ice-nucleating particle (INP) concentrations, in situ aerosol and cloud droplet number concentrations, and turbulence measurements in atmospheric vertical profiles. Moreover, concurrent measurements from a hilltop station were available as a reference for intercomparison; see Brus et al. (2025c) for details on the campaign setup.

In this study, we provide datasets of meteorological variables, aerosol concentrations, and size distributions collected during the intensive operation period (IOP) of the Pallas Cloud Experiment (PaCE 2022) campaign between 12 September and 10 October. Our dataset offers a unique opportunity for the broader scientific community to better understand the vertical structure of near-surface aerosol particles in a subarctic environment, revealing their crucial role in influencing low-level stratiform cloud microphysical and radiative properties. In Sect. 2, we describe the drone measurement platform and the assembly of the backpack module, including all of the sensors and their operational characteristics. Section 3 details the measurement sites, outlines the flight strategy, and presents the completed vertical profile measurements. Section 4 explains the dataset structure and the quality control and assurance of the data. Finally, Sect. 5 provides direct links to Zenodo dataset repository, which includes both netCDF and CSV files.

## 2 Description of the platform, module, and sensors

The FMI team operated a small, consumer-grade multicopter DJI Mavic 2 Pro drone with a custom-built measurement backpack mounted on top of the drone. The drone backpack is an entry-level air quality and atmospheric state measurement data acquisition system built around the Raspberry Pi Zero W microcomputer. It is intended to be used for air quality monitoring, vertical or horizontal profiling of the atmosphere, or any educational application in the field of aerosols or meteorology. The backpack utilizes a custom-designed drone-mounted sensor attachment system. The housing of the backpack is 3D-printed from a white polyethylene terephthalate glycol (PETG) filament material to reflect the Sun. The backpack is powered by a drone battery, and it is placed on top of the drone to minimize (to a high extent) the impact of the propeller airflow on the particulate matter (PM) measurements (e.g., Ghirardelli et al., 2023) while also still providing enough airflow around the sensors measuring atmospheric state variables, including temperature ($T$), relative humidity (RH), and pressure ($P$). The sensors are not force-aspirated; rather, the aspiration depends on the drone vertical movement and horizontal airflow for air exchange around the sensors. Typically, lightweight and small (size) sensors were used: BME280 for $T$, RH, and $P$ (Bosch Sensortec) and SHT85 for $T$ and RH (Sensirion AG). The backpack also included a GNSS module (Dual BN-220; Beitian Co. Ltd.) to retrieve redundancy positioning and the vertical and horizontal speed of the drone. The particulate matter (PM) sensor (OPC-N3, Alphasense Ltd.; e.g., Sousan et al., 2016; Crilley et al., 2018; Hagan and Kroll, 2020) was mounted on top of the backpack cover using zip ties; see Fig. 1. The PM sensor did not include any extra inlet or drying system for aerosol flow. The inlet was horizontal, facing towards the front of the drone. The sensors' measurement range and accuracy values are provided in Table 1. Estimates of wind speed and direction were calculated from the drone attitude, speed, and spatial orientation at each point of the flight. However, a third-party application, available at the https://airdata.com (last access: 3 October 2025) portal with a HD360 subscription, was used for wind estimates. In this paper, a proprietary wind algorithm (version 2.2) and the Mavic 2 Pro aerodynamic profile were used for wind estimates. The https://airdata.com application provided a wind map with a maximum of 5 s resolution, which corresponded to approximately 10–15 m in our vertical profile measurements. All sensors' variables were recorded to the Raspberry Pi at a 1 Hz resolution using dedicated, simple Python scripts.

## 3 Description of the measurement sites and completed vertical profiles

The Pallas Atmosphere–Ecosystem Supersite (https://en.ilmatieteenlaitos.fi/pallas-atmosphere-ecosystem-supersite, last access: 3 October 2025) is part of European Research Infrastructures and networks including ACTRIS (https://www.actris.eu/, last access: 3 October 2025), ICOS (https://www.icos-cp.eu/, last access: 3 October 2025), and EMEP and Global WMO GAW (https://wmo.int/activities/global-atmosphere-watch-programme-gaw, last access:

**Table 1.** An overview of the sensors (shown using italic font) and their operational characteristics provided by the manufacturers. Details on sensors' accuracy and tests can be found in following manufacturer data sheets: OPC-N3 (Alphasense Ltd., https://ametekcdn.azureedge.net/mediafiles/project/oneweb/oneweb/alphasense/products/datasheets/alphasense_opc-n3_datasheet_en_1.pdf?revision:29541b07-612a-42ba-b362-f41a48cf2e48, last access: 3 October 2025), BME280 (Bosch Sensortec GmbH, https://www.bosch-sensortec.com/media/boschsensortec/downloads/datasheets/bst-bme280-ds002.pdf, last access: 3 October 2025), and SHT85 (Sensirion AG, https://sensirion.com/resource/datasheet/sht85, last access: 3 October 2025).

| Sensor | Resolution | Accuracy | Range | Response time |
|---|---|---|---|---|
| *OPC, model N3* | | | | |
| Particle conc. ($cm^{-3}$) | $PM_1$, $PM_{2.5}$, and $PM_{10}$ mass concentrations $0.1\,\mu g\,m^{-3}$ | | $0–10^4$ particles $s^{-1}$<br>0.35–40 µm at 24 bins<br>Sample flow rate: 220 mL $min^{-1}$<br>Total flow rate: 5.5 L $min^{-1}$ | 1 s |
| *T* (°C) | | | −10 to 50 °C | |
| RH (%) | | | 0 %–95 % (non-condensing) | |
| *BME280* | | | | |
| *T* (°C) | 0.01 | ±0.5 °C | −40 to 85 °C | 1 s |
| RH (%) | < 0.01 | ±3 % | 0 %–100 % | 1 s at 25 °C |
| Pressure (hPa) | 0.18 Pa | ±1 hPa | 300–1100 hPa | 6 ms |
| *SHT85* | | | | |
| *T* (°C) | 0.01 | ±0.1 °C | −40 to 125 °C | 5 s |
| RH (%) | 0.01 | ±1.5 % | 0 %–100 % | 8 s at 25 °C and 1 m $s^{-1}$ airflow |
| *GPS*<br>*Beitian Dual BN-220* | Horizontal 2 m, vertical approx. 3 times horizontal | 0.1 m $s^{-1}$ | Chipset 8030-KT<br>Frequency: GPS L1, GLONASS L1, BeiDou B1, SBAS L1, Galileo<br>Timing: 1 µs synchronized to GPS time<br>Channels: 72 Searching Channel | Cold start: 26 s<br>Warm start: 25 s<br>Hot start: 1 s |

3 October 2025); for details on research programs, see, publications such as Lohila et al. (2015). There are no main emission sources close to the Pallas supersite. During the PaCE 2022 campaign, drone flights were carried out within the FMI Arctic UAV base reserved airspace – temporary dangerous area (TEMPO D – Pallas). The airspace is authorized for beyond-visual-line-of-sight (BVLOS) operations and covers a square region with a side length of approx. 14 km and an altitude ceiling limit of FL80 (∼ 2000 m a.g.l., above ground level). The area is centered on Sammaltunturi station, which is located above the treeline on the top of Sammaltunturi hill (67°58′24.0″ N, 24°06′56.3″ E; 560 m a.s.l., above sea level), approximately 300 m above the surrounding area. The station is commonly inside low-level clouds, especially during the autumn season. The drone flights were conducted at two relatively nearby locations: Pallasjärvi lake beach (68°01′23.2″ N, 24°09′48.8″ E; 276 m a.s.l.) and the UAV takeoff/landing site next to main road 957 in Pallaksentie (68°1′10.30″ N, 24°8′57.84″ E; 304 m a.s.l.). For details, see Fig. 2 and the map in Brus et al. (2025c). The intercomparison flights against reference instrumentation were done at Sammaltunturi station and next to the SMEAR 3 station measurement tower at Kumpula Campus in Helsinki (60°12.173′ N, 24°57.663′ E).

During the IOP of PaCE 2022, we flew missions focusing on the profiling of meteorological parameters and aerosol particles in size range of 0.35–40 µm. In total, we completed 63 vertical profile flights: 42 flights at Pallasjärvi lake beach, 21 flights next to main road 957 in Pallaksentie, and 12 flights against reference instrumentation at Sammaltunturi station (see Fig. 3). Only vertical profile data are included in the provided dataset. Our flight strategy was to conduct only high-resolution, strictly vertical flights and reach the maximum altitude of the DJI Mavic 2 Pro drone (500 m a.g.l). The flights were conducted with the OPC-N3 inlet always heading into the wind. The flight missions were conducted using the DJI GO 4 software, and both the ascent and descent rates were set to the same value (1 m $s^{-1}$). We aimed to perform vertical profiling whenever the weather allowed it, except on days with morning fog or precipitation at the site.

**Figure 1.** The DJI Mavic 2 Pro equipped with a drone air quality backpack.

Figure 4 provides the spatiotemporal variability in the measured meteorological variables and particle number concentration during the IOP of the PaCE 2022 campaign. The measured temperature spans from subzero values of −3 °C at 500 m a.g.l. to 15 °C at the surface. The RH and dew point exhibit wide variability throughout the measured column, with the RH ranging from 35 % to close to almost 90 %. Please note the bias in the RH when measured against the reference below (Fig. 5b). The particle number concentration ranged from very low values of 0.1 to about 300 $cm^{-3}$. These concentrations might include both aerosol and cloud particles, in the full size range from 0.3 to 40 µm (polystyrene latex (PSL) sphere equivalent) of the sensor, as the aerosol flow of the OPC-N3 was not dried.

## 4 Data processing and quality control

The data files generated by the drone backpack were formatted in NetCDF and CSV format. Quality control checks were applied, and missing data points or those with bad values were set to −9999.9. The files were named according to requirements depicted in Brus et al. (2025c), i.e., FMI.DBP.b1.yyyymmdd.hhmm.nc and FMI.DBP.b1.yyyymmdd.hhmm.csv, where DBP stands for drone backpack and yyyymmdd.hhmm corresponds to the date and time of the drone takeoff. These files include the Raspberry Pi real-time-clock time stamp (UTC); aircraft location (GNSS latitude and longitude in degrees and altitude in m a.s.l.); meteorological parameters measured by BME280 sensor, including temperature (°C), pressure (hPa), and relative humidity (%); and meteorological parameters measured by SHT85 sensor, including temperature (°C), relative humidity (%), dew point (°C), and estimated wind speed ($m\,s^{-1}$) and direction (°). Finally, these files include particle number concentrations ($cm^{-3}$) measured by the OPC-N3 sensor in 24 size bins with mid-bin diameters of 0.41, 0.56, 0.83, 1.15, 1.5, 2, 2.65, 3.5, 4.6, 5.85, 7.25, 9, 11, 13, 15, 17, 19, 21, 23.5, 26.5, 29.5, 32.5, 35.5, and 38.5 µm; the calculated total particle number concentration ($cm^{-3}$); the calculated $dN/d\log D_p$ ($cm^{-3}$) values in each size bin; and the measured $PM_1$, $PM_{2.5}$, and $PM_{10}$ mass concentrations (in $\mu g\,m^{-3}$). The PM values were calculated using the Alphasense Ltd. internal algorithm with the default setting for the OPC-N3, a refractive index of 1.5 (real part only), and a density of 1.65 $g\,cm^{-3}$. Additionally, the files provide temperature (°C), relative humidity (%), sample flow rate ($cm^3\,s^{-1}$), and the sampling period(s) of the sample flow. As the Raspberry Pi was not connected to the internet, its real-time clock was not synchronized with the GPS clock, causing a slight time lag between some parameters. This issue was resolved by adjusting the time using a lag calculation based on a cross-correlation between the measured pressure from the BME280 sensor (1 Hz) and the recorded altitude from the DJI Mavic 2 Pro (10 Hz); we estimate the maximum error in synchronization to be 1 s.

To estimate the uncertainty in the drone backpack measurements, we flew the drone backpack against the reference. We utilized continuous measurements at the Pallas Sammaltunturi station and the 30 m measurement tower of SMEAR 3 station at Kumpula Campus in Helsinki. The measurements at Pallas were done during the spring and autumn of 2022 to cover as wide a temperature and RH range as possible. The flights were done next to a 5 m high mast with a 3D anemometer and an automatic weather station (Milos 500, Vaisala Inc.). The measurements in Kumpula, Helsinki, were conducted in spring 2022 and compared against the 30 m high meteorological tower, which is equipped with meteorological instrumentation at several heights (4, 8, 16, and 30 m). However, intercomparison was done only at the 30 m level against an ultrasonic anemometer (Metek USA-1), a platinum resistance thermometer (Pt-100), and a thin-film polymer sensor (Vaisala DPA500). Further, the aerosol instrumentation for particulate measurements was placed on the FMI building roof, which is at the same height (30 m a.g.l.) and about 50 m (air distance) from the tower. The particulate matter intercomparison measurements were done against two optical particle counters (OPCs): the optical particle spectrometer (OPS model 3330, TSI Inc.), with a size range of 0.3–10 µm, and the mini cloud droplet analyzer (mCDA, Palas GmbH), with a size range of 0.35–17.6 µm. The drone hovered between the meteorological tower and the FMI building at Kumpula Campus. The horizontal inlet of the OPC-N3 placed on top of the drone backpack was always facing the wind direction to minimize the sampling losses due to non-isokinetic sampling (Julaha et al., 2025). The inlets of both reference OPCs were oriented vertically. The

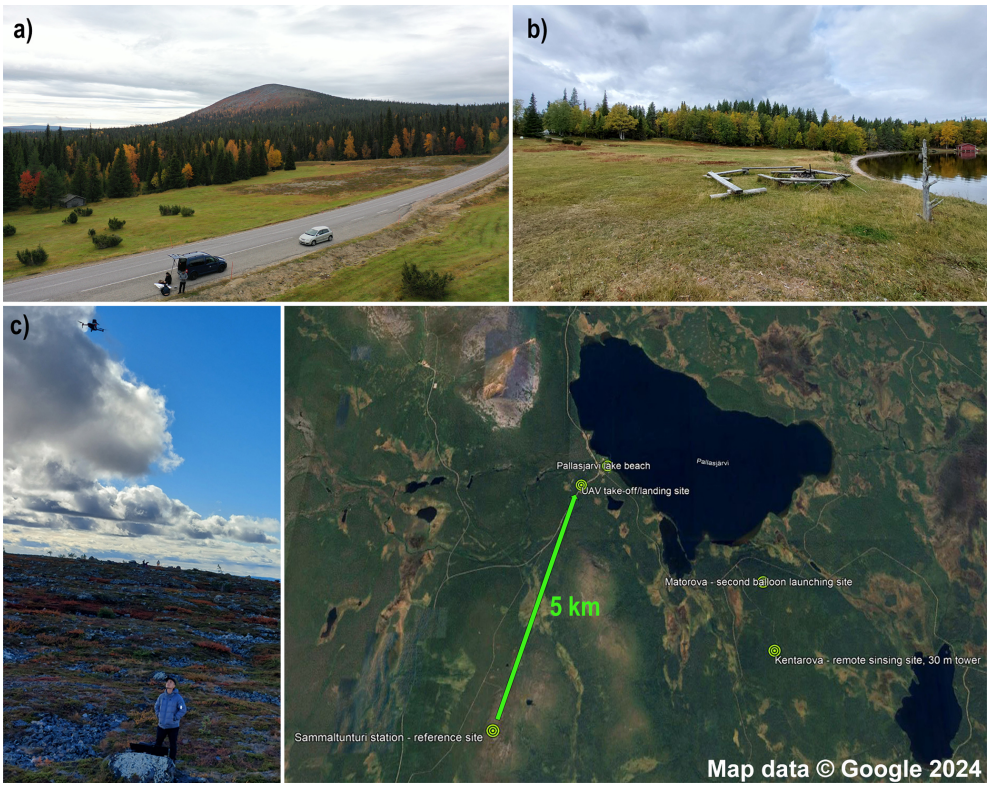


**Figure 2.** A map showing the locations of the sampling sites: **(a)** the UAV takeoff/landing site next to main road 957 at Pallaksentie (68°1′10.30″ N, 24°8′57.84″ E; 304 m a.s.l.), **(b)** Pallasjärvi lake beach (68°01′23.2″ N, 24°09′48.8″ E; 276 m a.s.l.), and **(c)** the calibration flight on the top of hill next to Sammaltunturi station (67°58′24.0″ N, 24°06′56.3″ E; 560 m a.s.l.). Background map courtesy of ©Google Maps.

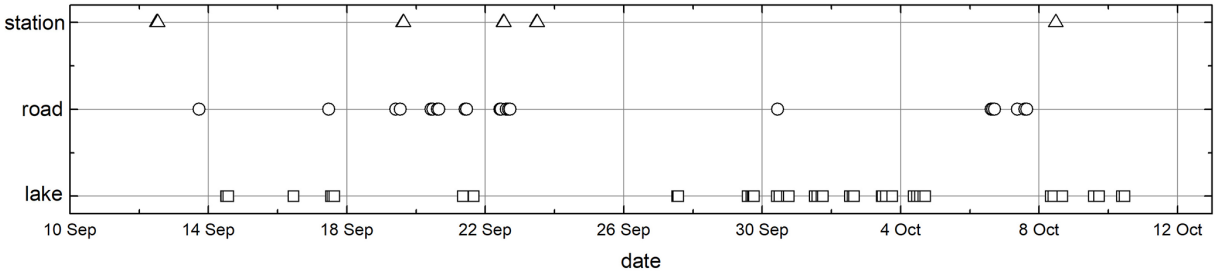


**Figure 3.** The timeline of DJI Mavic 2 Pro drone flight frequency at the three different locations.

measurements followed a consistent pattern: the drone took off from the ground and ascended to the height of the reference measurements. The drone was then oriented so that its front was heading into the wind. In GPS attitude flight mode, the drone hovered next to reference (at about 5 m horizontal distance) for at least 10 min at a low ambient temperature and for about 20 min at a higher ambient temperature, respectively. Data from both the drone backpack and reference instruments were averaged over the whole stably hovering period.

Figure 5 presents the intercomparison of meteorological variables measurements for (panel a) temperature, (panel b) RH, (panel c) wind speed, (panel d) wind direction, (panel e) dew point, and (panel f) pressure. The linear fit and the $R^2$ value are provided in each panel for each sensor separately. The drone backpack sensors' temperature measurements tended to slightly overestimate the reference measurements. The relative humidity measurements had the highest uncertainty (similarly to the findings of Barbieri et al., 2019): some measurements were done at very high ambient RH, and the sensors became saturated with water vapor and condensation occurred on sensor's surface. The third-party wind estimates from the drone attitude seem to have captured the wind direction more accurately than the wind speed. The

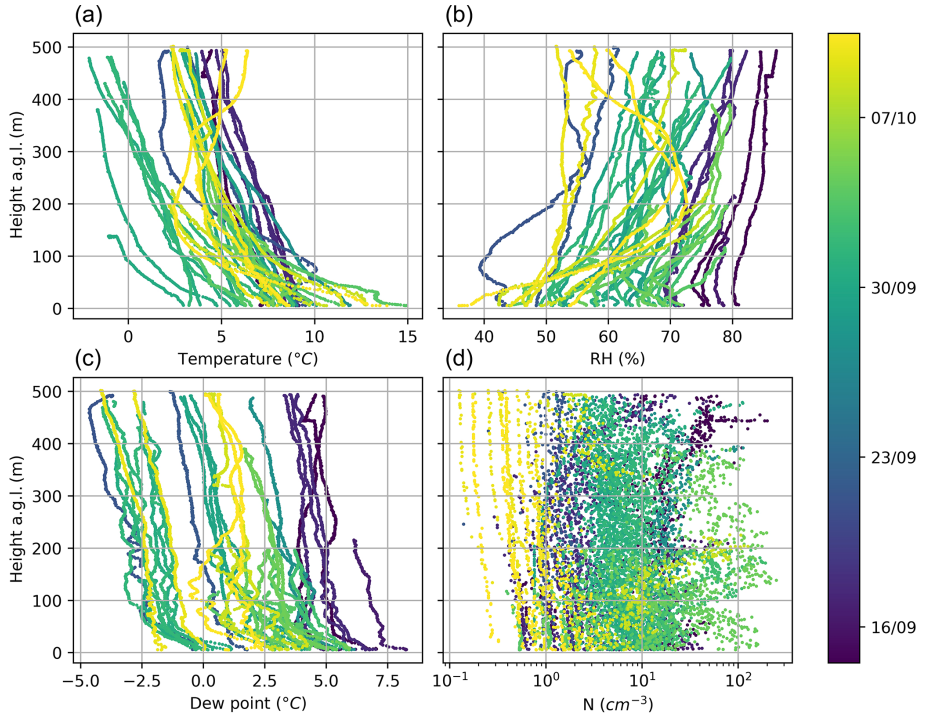


**Figure 4.** All measurement profiles of meteorological parameters: **(a)** temperature, **(b)** RH, **(c)** dew point, and **(d)** particle number concentration ($N$) collected during the IOP of PaCE 2022. Only ascending parts of the profiles are shown. The color scale represents the date of drone operation.

wind speed estimate has a positive bias of about $1\,m\,s^{-1}$ but reaches up to maximum of $2\,m\,s^{-1}$. It must be noted that it was not possible to get the wind speed and direction estimates for all flights due to a failure with respect to saving the drone attitude data to the drone flight controller. This problem was encountered in 10 out of 14 cases for Sammaltunturi station and 7 out of 16 case for the Kumpula reference flights. The dew point and pressure measurements follow the reference satisfactorily. However, it should be noted that the published dataset is at level b1 (i.e., data with quality control checks applied and missing data points or those with bad values were set to −9999.9) with no calibration factors applied, as specified in Brus et al. (2025c).

Figure 6a depicts the total particle concentration intercomparison of eight flights conducted in the first week of March 2022, while Fig. 6b shows the particle number size distribution. The particle number concentration is generally very low for the measured size range, up to $10\,cm^{-3}$. The variation in the particle concentration is naturally higher for OPC-N3 mounted on top of the drone backpack. We believe that this is due to external forces, like wind gusts or sudden changes in the wind direction, impacting the drone attitude and, thus, the particulate measurements. The particle number size distributions (only shown for three consecutive flights on 2 March 2022) of all OPCs follow the same shape, and the uncertainty in counting among the OPCs is about factor of 2, which is not unusual for drone aerosol measurements; see, e.g., Brus et al. (2021). Similarly to the meteorological variables, the particulate measurement dataset is at level b1 with no calibration factors applied.

### Dataset remarks

As hysteresis in the $T$ and RH profiles collected by the FMI drone backpack was noticeable, we recommend using only data from the ascending portion of the flight profiles. The descent data were found to be biased due to washout of the descending drone's propellers, and they exhibit a rather flat profile.

## 5 Data availability

Datasets collected by the FMI drone backpack were published on Zenodo (http://zenodo.org, last access: 5 February 2025) under the dedicated Pallas Cloud Experiment – PaCE2022 (https://zenodo.org/communities/pace2022/, last access: 5 February 2025) community archive as both NetCDF and CSV files: https://doi.org/10.5281/zenodo.14780929 (Brus et al., 2025a) and https://doi.org/10.5281/zenodo.14778421 (Brus et al., 2025b), respectively.

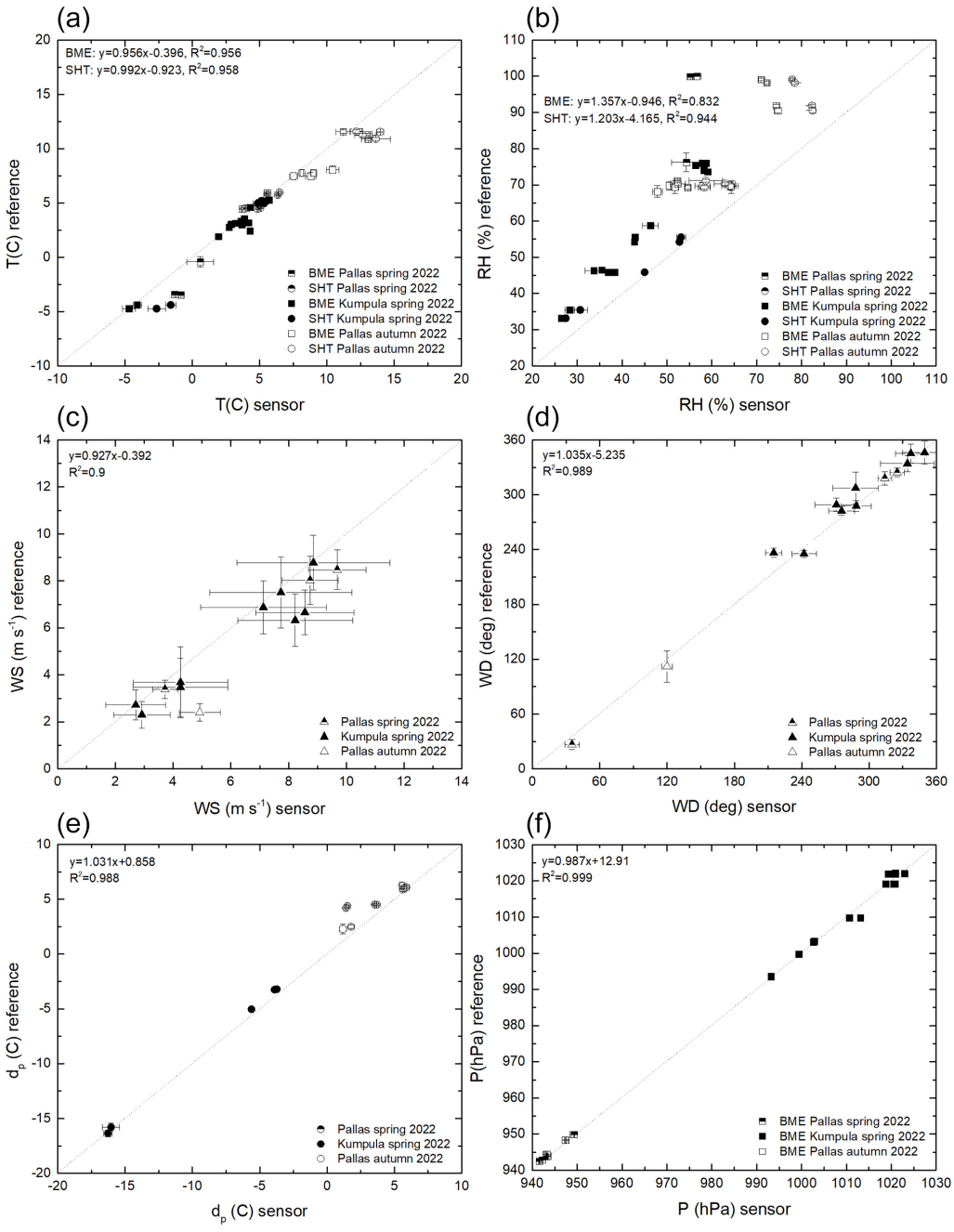


**Figure 5.** Drone backpack measurements against a reference at a given altitude for **(a)** temperature, **(b)** relative humidity, **(c)** wind speed, **(d)** wind direction, **(e)** dew point, and **(f)** pressure. The dotted line represents perfect agreement between the drone backpack and the reference instrumentation; it is included only to lead the readers' eyes. The linear fit with the $R^2$ value is depicted in each panel separately.

## 6 Code availability

The Python scripts developed to log, process, and display data are not publicly available; however, they can be accessed for free upon reasonable request to the authors.

## 7 Summary

This paper provides measurements and datasets collected by the FMI during the Pallas Cloud Experiment (PaCE 2022) campaign. The campaign took place in northern Finland during the autumn of 2022. In Sect. 2, we provide an overview of the platform deployed during this campaign and offer a payload description – the custom-built drone backpack for

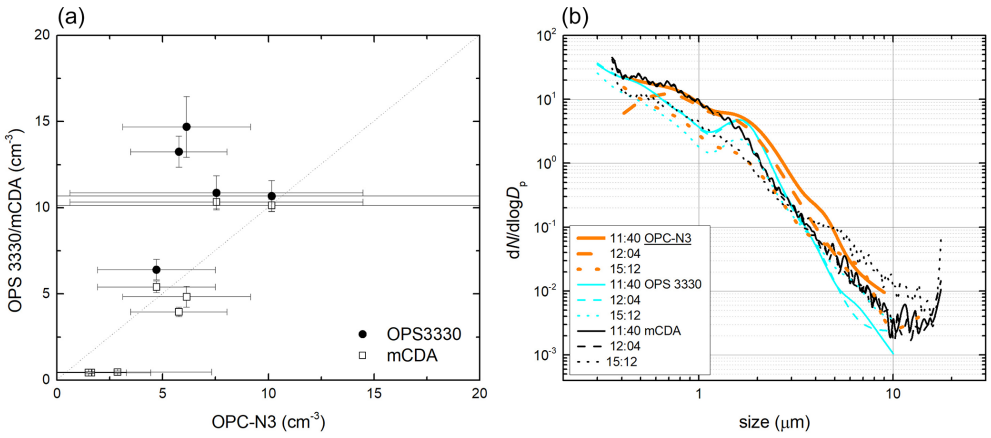


**Figure 6.** Drone backpack OPC-N3 particulate matter measurements against the reference instruments, the OPS (model 3330, TSI Inc.) and the mCDA (Palas GmbH). Panel **(a)** shows the total aerosol concentration, while panel **(b)** presents the particle number size distribution, both measured within the range of each instrument.

air quality and atmospheric state variable measurement carried on top of a consumer-grade drone (DJI Mavic 2 Pro). In Sect. 3, we describe the flight strategies, while Sect. 4 provides an overview of the datasets obtained, including a description of the measurements against the reference for data validation. Section 5 provides information on the dataset availability, and all files are available in both netCDF and CSV format.

During the PaCE 2022 campaign, different airborne platforms, including UAVs and tethered-balloon systems (TBSs), carrying various payloads for in situ aerosol and cloud physical property and atmospheric state variable measurements were deployed concurrently. Moreover, continuous surface in situ measurements of aerosol and cloud properties are available from the Sammaltunturi hilltop station; these could serve as a reference or as complementary information for further analysis. We encourage prospective users to integrate the drone backpack measurements with the comprehensive dataset of aerosol physical and optical properties from the hilltop station, as summarized by Backman et al. (2025). Specifically, the online ice-nucleating particle (INP) measurements presented by Böhmländer et al. (2025a) and the fluorescent aerosol measurements by Gratzl et al. (2025) offer a valuable complement. Further analysis and intercomparison of various sensor data can be conducted against other airborne measurements. These include fixed-wing UAV aerosol and cloud in situ measurements by Girdwood et al. (2025), UAV INP profiling by Böhmländer et al. (2025b), and tethered-balloon system (TBS) measurements covering turbulence and cloud microphysics by Schlenczek et al. (2025). Additionally, high-resolution TBS profiling of the boundary layer by Chávez-Medina et al. (2025) and aerosol and cloud measurements by Le et al. (2025) provide further avenues for comparative studies.

Moreover, aerosol properties below the cloud base can be analyzed using lidar backscatter, aerosol depolarization ratio, and turbulence parameters derived from the remote-sensing dataset presented by Tukiainen et al. (2025). All of the datasets from the "Data generated during the Pallas Cloud Experiment 2022 campaign" special issue of *Earth System Science Data* provide a comprehensive foundation for researchers investigating aerosol–cloud interactions and their dynamics.

**Author contributions.** DB planned and coordinated the FMI flights during the PaCE 2022 campaign; DB, VL, and KD conducted drone backpack measurements; VL and DB processed, analyzed, and quality-controlled the FMI dataset; and JK and DB designed the drone backpack. All authors contributed to the writing of the manuscript and quality-controlled the FMI dataset.

**Competing interests.** At least one of the (co-)authors is a guest member of the editorial board of *Earth System Science Data* for the special issue "Data generated during the Pallas Cloud Experiment 2022 campaign". The peer-review process was guided by an independent editor, and the authors also have no other competing interests to declare.

**Disclaimer.** Publisher's note: Copernicus Publications remains neutral with regard to jurisdictional claims made in the text, published maps, institutional affiliations, or any other geographical representation in this paper. While Copernicus Publications makes every effort to include appropriate place names, the final responsibility lies with the authors.

**Special issue statement.** This article is part of the special issue "Data generated during the Pallas Cloud Experiment 2022 campaign". It is not associated with a conference.

**Acknowledgements.** The authors would like to acknowledge Metsähallitus personnel, namely Mirka Hatanpää, for their unwavering support during the Pallas Cloud Experiment 2022.

**Financial support.** This work was supported by ACTRIS Finland funding through the Ministry of Transport and Communications, Atmosphere and Climate Competence Center Flagship funding by the Research Council of Finland (grant no. 337552). This project has also received funding from the European Union, H2020 Research and Innovation program (ACTRIS-IMP, the European Research Infrastructure for the observation of Aerosol, Clouds, and Trace gases; grant no. 871115).

**Review statement.** This paper was edited by Gholamhossein Bagheri and reviewed by Simon Thivet and Konrad Bärfuss.

## References

Abbatt, J. P. D., Leaitch, W. R., Aliabadi, A. A., Bertram, A. K., Blanchet, J.-P., Boivin-Rioux, A., Bozem, H., Burkart, J., Chang, R. Y. W., Charette, J., Chaubey, J. P., Christensen, R. J., Cirisan, A., Collins, D. B., Croft, B., Dionne, J., Evans, G. J., Fletcher, C. G., Galí, M., Ghahreman, R., Girard, E., Gong, W., Gosselin, M., Gourdal, M., Hanna, S. J., Hayashida, H., Herber, A. B., Hesaraki, S., Hoor, P., Huang, L., Hussherr, R., Irish, V. E., Keita, S. A., Kodros, J. K., Köllner, F., Kolonjari, F., Kunkel, D., Ladino, L. A., Law, K., Levasseur, M., Libois, Q., Liggio, J., Lizotte, M., Macdonald, K. M., Mahmood, R., Martin, R. V., Mason, R. H., Miller, L. A., Moravek, A., Mortenson, E., Mungall, E. L., Murphy, J. G., Namazi, M., Norman, A.-L., O'Neill, N. T., Pierce, J. R., Russell, L. M., Schneider, J., Schulz, H., Sharma, S., Si, M., Staebler, R. M., Steiner, N. S., Thomas, J. L., von Salzen, K., Wentzell, J. J. B., Willis, M. D., Wentworth, G. R., Xu, J.-W., and Yakobi-Hancock, J. D.: Overview paper: New insights into aerosol and climate in the Arctic, Atmos. Chem. Phys., 19, 2527–2560, https://doi.org/10.5194/acp-19-2527-2019, 2019.

Altstädter, B., Platis, A., Wehner, B., Scholtz, A., Wildmann, N., Hermann, M., Käthner, R., Baars, H., Bange, J., and Lampert, A.: ALADINA – an unmanned research aircraft for observing vertical and horizontal distributions of ultrafine particles within the atmospheric boundary layer, Atmos. Meas. Tech., 8, 1627–1639, https://doi.org/10.5194/amt-8-1627-2015, 2015.

Asmi, E., Kivekäs, N., Kerminen, V.-M., Komppula, M., Hyvärinen, A.-P., Hatakka, J., Viisanen, Y., and Lihavainen, H.: Secondary new particle formation in Northern Finland Pallas site between the years 2000 and 2010, Atmos. Chem. Phys., 11, 12959–12972, https://doi.org/10.5194/acp-11-12959-2011, 2011.

Backman, J., Luoma, K., Servomaa, H., Vakkari, V., and Brus, D.: In-situ aerosol measurements at the Arctic Sammaltunturi measurement station during the Pallas Cloud Experiment 2022, Earth Syst. Sci. Data Discuss. [preprint], https://doi.org/10.5194/essd-2025-284, in review, 2025.

Barbieri, L., Kral, S. T., Bailey, S. C. C., Frazier, A. E., Jacob, J. D., Reuder, J., Brus, D., Chilson, P. B., Crick, C., Detweiler, C., Doddi, A., Elston, J., Foroutan, H., González-Rocha, J., Greene, B. R., Guzman, M. I., Houston, A. L., Islam, A., Kemppinen, O., Lawrence, D., Pillar-Little, E. A., Ross, S. D., Sama, M. P., Schmale, D. G., Schuyler, T. J., Shankar, A., Smith, S. W., Waugh, S., Dixon, C., Borenstein, S., and de Boer, G.: Intercomparison of Small Unmanned Aircraft System (sUAS) Measurements for Atmospheric Science during the LAPSE-RATE Campaign, Sensors, 19, 2179, https://doi.org/10.3390/s19092179, 2019.

Böhmländer, A., Lacher, L., Fösig, R., Büttner, N., Nadolny, J., Brus, D., Doulgeris, K.-M., and Möhler, O.: Measurement of the ice-nucleating particle concentration with the Portable Ice Nucleation Experiment during the Pallas Cloud Experiment 2022, Earth Syst. Sci. Data Discuss. [preprint], https://doi.org/10.5194/essd-2025-89, in review, 2025a.

Böhmländer, A. J., Lacher, L., Höhler, K., Brus, D., Doulgeris, K.-M., Girdwood, J., Leisner, T., and Möhler, O.: Measurement of the ice-nucleating particle concentration using a mobile filter-based sampler on-board of a fixed-wing uncrewed aerial vehicle during the Pallas Cloud Experiment 2022, Earth Syst. Sci. Data Discuss. [preprint], https://doi.org/10.5194/essd-2025-87, in review, 2025b.

Brus, D., Gustafsson, J., Vakkari, V., Kemppinen, O., de Boer, G., and Hirsikko, A.: Measurement report: Properties of aerosol and gases in the vertical profile during the LAPSE-RATE campaign, Atmos. Chem. Phys., 21, 517–533, https://doi.org/10.5194/acp-21-517-2021, 2021.

Brus, D., Le, V., Kuula, J., and Doulgeris, K.: Data collected by a drone backpack for air quality and atmospheric state measurements during Pallas Cloud Experiment 2022 (PaCE2022), Zenodo [data set], https://doi.org/10.5281/zenodo.14780929, 2025a.

Brus, D., Le, V., Kuula, J., and Doulgeris, K.: Data collected by a drone backpack for air quality and atmospheric state measurements during Pallas Cloud Experiment 2022 (PaCE2022), Zenodo [data set], https://doi.org/10.5281/zenodo.14778421, 2025b.

Brus, D., Doulgeris, K., Bagheri, G., Bodenschatz, E., Chávez-Medina, V., Schlenczek, O., Khodamodari, H., Pohorsky, R., Schmale, J., Lonardi, M., Favre, L., Böhmländer, A., Möhler, O., Lacher, L., Girdwood, J., Gratzl, J., Grothe, H., Kaikkonen, V., Molkoselkä, E., Mäkynen, A., O'Connor, E., Leskinen, N., Tukiainen, S., Le, V., Backman, J., Luoma, K., Servomaa, H., and Asmi E.: Data generated during the Pallas Cloud Experiment 2022 campaign: an introduction and overview, Earth Syst. Sci. Data, in preparation, 2025c.

Coopman, Q., Riedi, J., Finch, D. P., and Garrett, T. J.: Evidence for changes in arctic cloud phase due to long-range pollution transport, Geophys. Res. Lett., 45, 10709–10718, https://doi.org/10.1029/2018GL079873, 2018.

Crilley, L. R., Shaw, M., Pound, R., Kramer, L. J., Price, R., Young, S., Lewis, A. C., and Pope, F. D.: Evaluation of a low-cost optical particle counter (Alphasense OPC-N2) for ambient air monitoring, Atmos. Meas. Tech., 11, 709–720, https://doi.org/10.5194/amt-11-709-2018, 2018.

de Boer, G., Diehl, C., Jacob, J., Houston, A., Smith, S. W., Chilson, P., Schmale III, D. G., Intrieri, J., Pinto, J., Elston, J., Brus, D., Kemppinen, O., Clark, A., Lawrence, D., Bailey, S. C. C., Sama, M. P., Frazier, A., Crick, C., Natalie, V., Pillar-Little, E., Klein, P., Waugh, S., Lundquist, J. K., Barbieri, L., Kral, S. T., Jensen, A. A., Dixon, C., Borenstein, S., Hesselius, D., Human, K., Hall, P., Argrow, B., Thornberry, T., Wright, R., and Kelly, J. T.: Development of community, capabilities and understand-

ing through unmanned aircraft-based atmospheric research: The LAPSE-RATE campaign, B. Am. Meteorol. Soc., 101, E684–E699, https://doi.org/10.1175/BAMS-D-19-0050.1, 2020.

Doulgeris, K. M., Vakkari, V., O'Connor, E. J., Kerminen, V.-M., Lihavainen, H., and Brus, D.: Influence of air mass origin on microphysical properties of low-level clouds in a subarctic environment, Atmos. Chem. Phys., 23, 2483–2498, https://doi.org/10.5194/acp-23-2483-2023, 2023.

Girdwood, J., Stanley, W., Stopford, C., and Brus, D.: Simulation and field campaign evaluation of an optical particle counter on a fixed-wing UAV, Atmos. Meas. Tech., 15, 2061–2076, https://doi.org/10.5194/amt-15-2061-2022, 2022.

Girdwood, J., Brus, D., Doulgeris, K.-M., and Böhmländer, A.: Small Uncrewed Aircraft Based Microphysical Measurements of Polar Stratus Cloud During The Pallas Cloud Experiment 2022, Earth Syst. Sci. Data Discuss. [preprint], https://doi.org/10.5194/essd-2025-257, in review, 2025.

Ghirardelli, M., Kral, S. T., Müller, N. C., Hann, R., Cheynet, E., and Reuder, J.: Flow Structure around a Multicopter Drone: A Computational Fluid Dynamics Analysis for Sensor Placement Considerations, Drones, 7, 467, https://doi.org/10.3390/drones7070467, 2023.

Gratzl, J., Brus, D., Doulgeris, K., Böhmländer, A., Möhler, O., and Grothe, H.: Fluorescent aerosol particles in the Finnish sub-Arctic during the Pallas Cloud Experiment 2022 campaign, Earth Syst. Sci. Data, 17, 3975–3985, https://doi.org/10.5194/essd-17-3975-2025, 2025.

Hagan, D. H. and Kroll, J. H.: Assessing the accuracy of low-cost optical particle sensors using a physics-based approach, Atmos. Meas. Tech., 13, 6343–6355, https://doi.org/10.5194/amt-13-6343-2020, 2020.

Chávez-Medina, V., Khodamoradi, H., Schlenczek, O., Nordsiek, F., Brunner, C. E., Bodenschatz, E., and Bagheri, G.: Max Planck WinDarts: High-Resolution Atmospheric Boundary Layer Measurements with the Max Planck CloudKite platform and Ground Weather Station – A Data Overview, Earth Syst. Sci. Data Discuss. [preprint], https://doi.org/10.5194/essd-2025-111, in review, 2025.

Jokinen, T., Lehtipalo, K., Thakur, R. C., Ylivinkka, I., Neitola, K., Sarnela, N., Laitinen, T., Kulmala, M., Petäjä, T., and Sipilä, M.: Measurement report: Long-term measurements of aerosol precursor concentrations in the Finnish subarctic boreal forest, Atmos. Chem. Phys., 22, 2237–2254, https://doi.org/10.5194/acp-22-2237-2022, 2022.

Julaha, K., Ždímal, V., Mbengue, S., Brus, D., and Zíková, N.: Drone-based vertical profiling of particulate matter size distribution and carbonaceous aerosols: urban vs. rural environment, EGUsphere [preprint], https://doi.org/10.5194/egusphere-2025-1420, 2025.

Kral, S. T., Reuder, J., Vihma, T., Suomi, I., Haualand, K. F., Urbancic, G. H., Greene, B. R., Steeneveld, G., Lorenz, T., Maronga, B., Jonassen, M. O., Ajosenpää, H., Båserud, L., Chilson, P. B., Holtslag, A. A. M., Jenkins, A. D., Kouznetsov, R., Mayer, S., Pillar-Little, E. A., Rautenberg, A., Schwenkel, J., Seidl, A. W., and Wrenger, B. : The Innovative Strategies for Observations in the Arctic Atmospheric Boundary Layer Project (ISOBAR): Unique Finescale Observations under Stable and Very Stable Conditions, B. Am. Meteorol. Soc., 102, E218–E243, https://doi.org/10.1175/BAMS-D-19-0212.1, 2021.

Kyrö, E.-M., Väänänen, R., Kerminen, V.-M., Virkkula, A., Petäjä, T., Asmi, A., Dal Maso, M., Nieminen, T., Juhola, S., Shcherbinin, A., Riipinen, I., Lehtipalo, K., Keronen, P., Aalto, P. P., Hari, P., and Kulmala, M.: Trends in new particle formation in eastern Lapland, Finland: effect of decreasing sulfur emissions from Kola Peninsula, Atmos. Chem. Phys., 14, 4383–4396, https://doi.org/10.5194/acp-14-4383-2014, 2014.

Le, V., Doulgeris, K. M., Komppula, M., Backman, J., Bagheri, G., Bodenschatz, E., and Brus, D.: Dataset of airborne measurements of aerosol, cloud droplets and meteorology by tethered balloon during PaCE 2022, Earth Syst. Sci. Data Discuss. [preprint], https://doi.org/10.5194/essd-2025-148, 2025.

Liu, B., Wu, C., Ma, N., Chen, Q., Li, Y., Ye, J., Martin, S. T., and Li, Y. J.: Vertical profiling of fine particulate matter and black carbon by using unmanned aerial vehicle in Macau, China, Sci. Total Environ., 709, 136109, https://doi.org/10.1016/j.scitotenv.2019.136109, 2020.

Liu, J. and Li, Z.: Aerosol properties and their influences on low warm clouds during the Two-Column Aerosol Project, Atmos. Chem. Phys., 19, 9515–9529, https://doi.org/10.5194/acp-19-9515-2019, 2019.

Lohila, A., Penttilä, T., Jortikka, S., Aalto, T., Anttila, P., Asmi, E., Aurela, M., Hatakka, J., Hellén, H., Henttonen, H., Hänninen, P., Kilkki, J., Kyllönen, K., Laurila, T., Lepistö, A., Lihavainen, H., Makkonen, U., Paatero, J., Rask, M., Sutinen, R., Tuovinen, J.-P., Vuorenmaa, J., and Viisanen, Y.: Preface to the special issue on integrated research of atmosphere, ecosystems and environment at Pallas, Boreal Environ. Res., 20, 431–454, 2015.

Morrison, H., van Lier-Walqui, M., Fridlind, A. M., Grabowski, W. W., Harrington, J. Y., Hoose, C., Korolev, A., Kumjian, M. R., Milbrandt, J. A., Pawlowska, H., Posselt, D. J., Prat, O. P., Reimel, K. J., Shima, S.-I., van Diedenhoven, B., and Xueet, L.: Confronting the challenge of modeling cloud and precipitation microphysics, J. Adv. Model. Earth Sy., 12, e2019MS001689, https://doi.org/10.1029/2019MS001689, 2020.

Pasquier, J., David, R., Freitas, G., Gierens, R., Gramlich, Y., Haslett, S., Li, G., Schäfer, B., Siegel, K., Wieder, J., Adachi, K., Belosi, F., Carlsen, T., Decesari, S., Ebell, K., Gilardoni, S., Gysel-Beer, M., Henneberger, J., Inoue, J., Kanji, Z., Koike, M., Kondo, Y., Krejci, R., Lohmann, U., Maturilli, M., Mazzolla, M., Modini, R., Mohr, C., Motos, G., Nenes, A., Nicosia, A., Ohata, S., Paglione, M., Park, S., Pileci, R., Ramelli, F., Rinaldi, M., Ritter, C., Sato, K., Storelvmo, T., Tobo, Y., Traversi, R., Viola, A., and Zieger, P.: The Ny-Ålesund Aerosol Cloud Experiment (NASCENT): Overview and First Results, B. Am. Meteorol. Soc., 103, E2533–E2558, 2022.

Samad, A., Vogt, U., Panta, A., and Uprety, D.: Vertical distribution of particulate matter, black carbon and ultra-fine particles in Stuttgart, Germany, Atmos. Pollut. Res., 11, 1441–1450, https://doi.org/10.1016/j.apr.2020.05.017, 2020.

Schlenczek, O., Nordsiek, F., Brunner, C. E., Chávez-Medina, V., Thiede, B., Bodenschatz, E., and Bagheri, G.: Airborne measurements of turbulence and cloud microphysics during PaCE 2022 using the Advanced Max Planck CloudKite Instrument (MPCK+), Earth Syst. Sci. Data Discuss. [preprint], https://doi.org/10.5194/essd-2025-112, in review, 2025.

Schmale, J., Sharma, S., Decesari, S., Pernov, J., Massling, A., Hansson, H.-C., von Salzen, K., Skov, H., Andrews, E., Quinn, P. K., Upchurch, L. M., Eleftheriadis, K., Traversi, R., Gilar-

doni, S., Mazzola, M., Laing, J., and Hopke, P.: Pan-Arctic seasonal cycles and long-term trends of aerosol properties from 10 observatories, Atmos. Chem. Phys., 22, 3067–3096, https://doi.org/10.5194/acp-22-3067-2022, 2022.

Sedlar, J., Tjernström, M., Rinke, A., Orr, A., Cassano, J., Fettweis, X., Heinemann, G., Seefeldt, M., Solomon, A., Matthes, H., Phillips, T., and Webster, S.: Confronting Arctic troposphere, clouds, and surface energy budget representations in regional climate models with observations, J. Geophys. Res.-Atmos., 125, https://doi.org/10.1029/2019JD031783, 2020.

Sousan, S., Koehler, K., Hallett, L., and Peters, T. M.: Evaluation of the Alphasense Optical Particle Counter (OPC-N2) and the Grimm Portable Aerosol Spectrometer (PAS-1.108), Aerosol Sci. Tech., 50, 1352–1365, https://doi.org/10.1080/02786826.2016.1232859, 2016.

Stevens, R. G., Loewe, K., Dearden, C., Dimitrelos, A., Possner, A., Eirund, G. K., Raatikainen, T., Hill, A. A., Shipway, B. J., Wilkinson, J., Romakkaniemi, S., Tonttila, J., Laaksonen, A., Korhonen, H., Connolly, P., Lohmann, U., Hoose, C., Ekman, A. M. L., Carslaw, K. S., and Field, P. R.: A model intercomparison of CCN-limited tenuous clouds in the high Arctic, Atmos. Chem. Phys., 18, 11041–11071, https://doi.org/10.5194/acp-18-11041-2018, 2018.

Thivet, S., Bagheri, G., Kornatowski, P. M., Fries, A., Lemus, J., Simionato, R., Díaz-Vecino, C., Rossi, E., Yamada, T., Scollo, S., and Bonadonna, C.: In situ volcanic ash sampling and aerosol–gas analysis based on UAS technologies (AeroVolc), Atmos. Meas. Tech., 18, 2803–2824, https://doi.org/10.5194/amt-18-2803-2025, 2025.

Tukiainen, S., Siipola, T., Leskinen, N., and O'Connor, E.: Remote sensing measurements during PaCE 2022 campaign, Earth Syst. Sci. Data, 17, 3797–3806, https://doi.org/10.5194/essd-17-3797-2025, 2025.

Zhu, Y., Wu, Z., Park, Y., Fan, X., Bai, D., Zong, P., Qin, B., Cai, X., and Ahn, K.-H.: Measurements of atmospheric aerosol vertical distribution above North China Plain using hexacopter, Sci. Total Environ., 665, 1095–1102, https://doi.org/10.1016/j.scitotenv.2019.02.100, 2019.